J|A|C|S
ARTICLES
Published on Web 10/23/2007

A Stroboscopic Approach for Fast Photoactivation−Localization Microscopy with Dronpa Mutants

Cristina Flors,[†] Jun-ichi Hotta,[†] Hiroshi Uji-i,[†] Peter Dedecker,[†] Ryoko Ando,[‡] Hideaki Mizuno,[‡] Atsushi Miyawaki,[‡] and Johan Hofkens*,[†]

Contribution from the Department of Chemistry and Institute for Nanoscale Physics and Chemistry (INPAC), Katholieke Universiteit Leuven, Celestijnenlaan 200F, 3001 Heverlee, Belgium, and Laboratory for Cell Function and Dynamics, Brain Science Institute, RIKEN, 2-1 Hirosawa, Wako, Saitama 351-0198, Japan

Received June 27, 2007; E-mail: johan.hofkens@chem.kuleuven.be

Abstract: The photophysical properties and photoswitching scheme of the reversible photoswitchable green fluorescent protein-like fluorescent proteins Dronpa-2 and Dronpa-3 were investigated by means of ensemble and single-molecule fluorescence spectroscopy and compared to those of the precursor protein Dronpa. The faster response to light and the faster dark recovery of the new mutants observed in bulk also hold at the single-molecule level. Analysis of the single-molecule traces allows us to extract the efficiencies and rate constants of the pathways involved in the forward and backward switching, and we find important differences when comparing the mutants to Dronpa. We rationalize our results in terms of a higher conformational freedom of the chromophore in the protein environment provided by the β-can. This thorough understanding of the photophysical parameters has allowed us to optimize the acquisition parameters for camera-based sub-diffraction-limit imaging with these photochromic proteins. We show that Dronpa and its mutants are useful for fast photoactivation−localization microscopy (PALM) using common wide-field microscopy equipment, as individual fluorescent proteins can be localized several times. We provide a new approach to achieve fast PALM by introducing simultaneous two-color stroboscopic illumination.

Introduction

A wide range of fluorescent proteins have been used as genetically encodable markers that allow non-invasive analysis of protein localization and dynamics in living cells.[1−5] A rather recent group within these proteins are the green fluorescent protein (GFP)-like photoswitchable proteins, or "optical highlighters", which can be converted from a fluorescent "on" state to a non-fluorescent "off" state or vice versa.[6−8] Of particular interest are the proteins that are able to photoswitch in a reversible fashion.[9−12] Among the latter, Dronpa, a mutant of a GFP-like protein derived from coral Pectiniidae,[12] is one of the most promising candidates available at present. Its significance stems from its fast response to light for the forward and especially for the backward photoswitching reaction and its highly reliable reversibility. Moreover, the fact that it is monomeric allows its use for tracking individual intracellular molecules and for designing fluorescence resonance energy transfer experiments. The fluorescent (anionic, deprotonated) and non-fluorescent (neutral, protonated) states of Dronpa show absorption bands at 503 and 388 nm, respectively. Photoswitching from the dark to the bright state involves deprotonation of the chromophore,[13] although photoisomerization has also been proposed to play a role.[14,15] Very recently, new mutants of Dronpa have been developed by semi-random[16] and site-directed[15] mutagenesis. These interesting mutants are characterized by a faster response to 488-nm light for the forward

[†] Katholieke Universiteit Leuven.
[‡] Brain Science Institute, RIKEN.

(1) Lippincott-Schwartz, J.; Patterson, G. H. *Science* **2003**, *300*, 87−91.
(2) Chudakov, D. M.; Lukyanov, S.; Lukyanov, K. A. *Trends Biotechnol.* **2005**, *23*, 605−613.
(3) Miyawaki, A.; Sawano, A.; Kogure, T. *Nat. Cell. Biol.* **2003**, Suppl., S1−S7.
(4) Shaner, N. C.; Steinbach, P. A.; Tsien, R. Y. *Nat. Methods* **2005**, *2*, 905−909.
(5) Remington, S. J. *Curr. Opin. Struct. Biol.* **2006**, *16*, 714−721.
(6) Wiedenmann, J.; Nienhaus, G. U. *Expert Rev. Proteomics* **2006**, *3*, 361−374.
(7) Lukyanov, K. A.; Chudakov, D. M.; Lukyanov, S.; Verkhusha, V. V. *Nat. Rev. Mol. Cell Biol.* **2005**, *6*, 885−891.
(8) Chapman, S.; Oparka, K. J.; Roberts, A. G. *Curr. Opin. Plant Biol.* **2005**, *8*, 565−573.
(9) Andresen, M.; Wahl, M. C.; Stiel, A. C.; Grater, F.; Schafer, L. V.; Trowitzsch, S.; Weber, G.; Eggeling, C.; Grubmuller, H.; Hell, S. W.; Jakobs, S. *Proc. Natl. Acad. Sci. U.S.A.* **2005**, *102*, 13070−13074.
(10) Chudakov, D. M.; Belousov, V. V.; Zaraisky, A. G.; Novoselov, V. V.; Staroverov, D. B.; Zorov, D. B.; Lukyanov, S.; Lukyanov, K. A. *Nat. Biotechnol.* **2003**, *21*, 191−194.
(11) Lukyanov, K.; Fradkov, A.; Gurskaya, N.; Matz, M.; Labas, Y.; Savitsky, A.; Markelov, M.; Zaraisky, A.; Zhao, X.; Fang, Y.; Tan, W.; Lukyanov, S. *J. Biol. Chem.* **2000**, *275*, 25879−25882.
(12) Ando, R.; Mizuno, H.; Miyawaki, A. *Science* **2004**, *306*, 1370−1373.
(13) Fron, E.; Flors, C.; Schweitzer, G.; Habuchi, S.; Mizuno, H.; Ando, R.; Miyawaki, A.; de Schryver, F. C.; Hofkens, J. *J. Am. Chem. Soc.* **2007**, *129*, 4870−4871.
(14) Andresen, M.; Stiel, A. C.; Trowitzsch, S.; Weber, G.; Eggeling, C.; Wahl, M. C.; Hell, S. W.; Jakobs, S. *Proc. Natl. Acad. Sci. U.S.A.* **2007**, *104*, 13005−13009.
(15) Stiel, A. C.; Trowitzsch, S.; Weber, G.; Andresen, M.; Eggeling, C.; Hell, S. W.; Jakobs, S.; Wahl, M. C. *Biochem. J.* **2007**, *402*, 35−42.
(16) Ando, R.; Flors, C.; Mizuno, H.; Hofkens, J.; Miyawaki, A. *Biophys. J.* **2007**, *92*, L97−L99.

10.1021/ja074704l CCC: $37.00

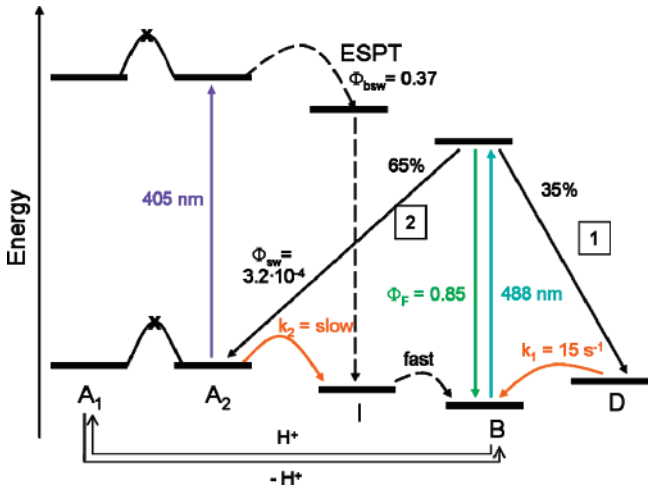

Figure 1. Photoconversion scheme for Dronpa.[17] ESPT = excited-state proton transfer; the definitions for the other symbols are given in the text.

photoswitching reaction and by a faster thermal relaxation from the "off" to the "on" state.

The reversible photoswitching of Dronpa was shown to hold at the single-molecule level, with an individual protein being able to undergo more than 100 photocycles.[17,18] Furthermore, single-molecule experiments gave insight into the mechanism underlying the photoswitching. The analysis of fluorescence trajectories of individual Dronpa molecules revealed on−off dynamics on two different time scales, seconds and tens of milliseconds, and allowed the proposal of a photoconversion scheme (Figure 1). According to this scheme, protonation of an anionic fluorescent state (B) to form a photoswitched non-fluorescent protonated form (A_2) occurs after prolonged irradiation of B at 488 nm. The recovery of the "on" state (B) can be thermal (k_2) or activated by 405-nm light, involving in both cases a non-fluorescent intermediate I, thought to be a deprotonated form in an unrelaxed protein environment. In addition, another dark intermediate D was hypothesized, which may account for the blinking dynamics in the tens of milliseconds time range.[17] It appears that the pH-induced protonated form (A_1) and the photoswitched protonated form (A_2) are not interconvertible, although they are spectroscopically very similar.[12] However, in the excited state, their differences become more evident.[13]

One of the most promising applications of Dronpa and other fluorescent proteins is their use in obtaining an improved, nanoscale resolution in fluorescence microscopy.[19−23] To date, several approaches have taken advantage of the photoswitchable properties of fluorescent proteins (and other fluorophores), namely those based on zero-intensity-based read-out (RESOLFT[24]) or on stochastic photoactivation and localization of single molecules (PALM,[25] FPALM,[26] STORM[27]). The latter methods are based on cycles of stochastic on/off switching of the fluorescence emission, where fluorescence can only be registered for those molecules that are in the "on" state during a particular cycle. Within a given cycle, the activated molecules should be well enough separated from each other (farther apart than the distance resolved by the microscope). It is then possible to localize with high precision the centroids of the individual fluorescent signals for each cycle and to construct a sub-diffraction-limit image of the sample, incorporating all the centroid positions of all the cycles. Moreover, this can be readily extended to the simultaneous localization of two or more different types of fluorophores with different emission wavelengths.[28] In this paper, we show that the fluorescence photoswitching of Dronpa and its mutants is useful for stochastic sub-diffraction-limit microscopy and that a detailed knowledge of their photophysical properties is indispensable for the optimization of the acquisition parameters. We have studied Dronpa-2 and Dronpa-3, which carry the mutations Met159Thr and Val157Ile/Met159Ala, respectively,[16] by means of ensemble and single-molecule spectroscopy, and we compare them to the precursor Dronpa. We report on fast sub-diffraction-limit imaging with these fluorescent proteins. Due to the fast switching of the studied mutants, we developed a new approach to photoactivation−localization microscopy (PALM) that involves two-color stroboscopic illumination (S-PALM). Furthermore, by using 50-nm objects, we provide an estimation of the quality and resolution improvement of the reconstructed images.

Materials and Methods

Sample Preparation. Dronpa, Dronpa-2, and Dronpa-3 were expressed and purified as described previously.[12,16] Ensemble experiments were performed in phosphate-buffered saline (PBS) solution (10 mM KH_2PO_4/10 mM K_2HPO_4/138 mM NaCl, 2.7 mM KCl, pH 7.4, Sigma, St. Louis, MO). Spheres coated with fluorescent proteins that were used for demonstration of photoactivation−localization microscopy were prepared by incubating non-fluorescent neutravidin-labeled nanospheres (43 nm, F8772, Molecular Probes) with biotinylated fluorescent proteins (∼1 h at 4 °C). Biotinylated fluorescent proteins were prepared by incubating (∼1 h at 4 °C) His-tagged fluorescent proteins with a biotinylated antibody to His tag (SM1693B, Acris Antibodies), followed by dialysis (100 kDa MW cutoff, 24 h at 4 °C, PBS pH 7.4). The total size of the sphere is estimated as ∼50 nm diameter, including the fluorescent proteins and the antibody. There are ∼85 binding sites in the spheres,[29] so a maximum of ∼170 fluorescent proteins can be attached to one sphere (if we assume two fluorescent proteins per antibody). Samples for microscopy were prepared by spin-coating the proteins or the spheres (∼10^{-11} M in PBS containing 1% (wt) poly(vinyl alcohol) (PVA)) on a cover glass at 3000 rpm.[17]

Ensemble Spectroscopy. Steady-state absorption and emission spectra were recorded on a Lambda 40 spectrophotometer (Perkin-Elmer, Wellesley, MA) and a Fluorolog 1500 fluorimeter (Spex Industries, Metuchen, NJ), respectively. The time-correlated single-photon counting (TCSPC) method was used to measure time-resolved fluorescence decays, with excitation at 484 nm (1.2 ps, 4.09 MHz) provided by a Ti:sapphire laser (Tsunami, Spectra Physics, Mountain

(17) Habuchi, S.; Ando, R.; Dedecker, P.; Verheijen, W.; Mizuno, H.; Miyawaki, A.; Hofkens, J. *Proc. Natl. Acad. Sci. U.S.A.* **2005**, *102*, 9511−9516.
(18) Habuchi, S.; Dedecker, P.; Hotta, J.; Flors, C.; Ando, R.; Mizuno, H.; Miyawaki, A.; Hofkens, J. *Photochem. Photobiol. Sci.* **2006**, *5*, 567−576.
(19) Sauer, M. *Proc. Natl. Acad. Sci. U.S.A.* **2005**, *102*, 9433−9434.
(20) Gustafsson, M. G. *Proc. Natl. Acad. Sci. U.S.A.* **2005**, *102*, 13081−13086.
(21) Irie, M.; Fukaminato, T.; Sasaki, T.; Tamai, N.; Kawai, T. *Nature* **2002**, *420*, 759−760.
(22) Enderlein, J. *Appl. Phys. Lett.* **2005**, *87*, 097105.
(23) Hell, S. W. *Science* **2007**, *316*, 1153−1158.
(24) Hofmann, M.; Eggeling, C.; Jakobs, S.; Hell, S. W. *Proc. Natl. Acad. Sci. U.S.A.* **2005**, *102*, 17565−17569.
(25) Betzig, E.; Patterson, G. H.; Sougrat, R.; Lindwasser, O. W.; Olenych, S.; Bonifacino, J. S.; Davidson, M. W.; Lippincott-Schwartz, J.; Hess, H. F. *Science* **2006**, *313*, 1642−1645.
(26) Hess, S. T.; Girirajan, T. P. K.; Mason, M. D. *Biophys. J.* **2006**, *91*, 4258−4272.
(27) Rust, M. J.; Bates, M.; Zhuang, X. W. *Nat. Methods* **2006**, *3*, 793−795.
(28) Bock, H.; Geisler, C.; Wurm, C. A.; von Middendorff, C.; Jakobs, S.; Schonle, A.; Egner, A.; Hell, S. W.; Eggeling, C. *Appl. Phys. B* **2007**, *88*, 161−165.
(29) Allen, N. W.; Thompson, N. L. *Cytometry* **2006**, *69A*, 524−532.

View, CA). The details of the experimental setup and the data acquisition have been described previously.[30] In the TCSPC experiments, the sample was flowed through a 1-cm optical path cuvette by means of a peristaltic pump. For the activation energy determination, the temperature of the samples was controlled with a thermoelectric temperature controller (LFI-3751, Wavelength Electronics, Bozeman, MT).

Single-Molecule Confocal Scanning Microscopy. Samples were mounted on an inverted microscope (IX-70, Olympus, Tokyo, Japan) equipped with a scanning stage (Physik Instrumente, Karlsruhe/Palmbach, Germany). Circularly polarized 488-nm light from a continuous-wave (CW) Ar−Kr ion laser (Stabilite 2018-RM, Spectra Physics) was introduced into the microscope and focused by an oil immersion objective lens (Olympus, numerical aperture 1.3, ×100). For two-color excitation measurements, the CW 488- and 405-nm (Compass 405-25, Coherent, Santa Clara, CA) laser light was introduced coaxially into the microscope. Fluorescence was collected by the same objective, passed through a dichroic mirror (495DCLP, Chroma Technology, Rockingham, VT), a notch filter (488 nm, Kaiser Optical Systems, Ann Arbor, MI), and long-pass filters (450LP, 505LP, Chroma Technology), and focused through a 100-μm pinhole to an avalanche photodiode (SPCM-AQR-14, Perkin-Elmer, Waltham, MA). Fluorescence from single fluorescent proteins was registered by a TCSPC card (SPC 630, Becker & Hickl, Berlin, Germany) using the first-in, first-out (FIFO) mode.[31] All single-molecule experiments were performed at room temperature.

Photoactivation−Localization Microscopy. The wide-field fluorescent microscope consisted of an inverted optical microscope (IX71, Olympus) equipped with a 1.3-numerical aperture, 100× oil immersion objective (UPlanFLN, Olympus) and a highly sensitive cooled electron multiplying charge-coupled device (CCD) camera with 512 × 512 pixels (iXon, Andor Technology, South Windsor, CT) with a pixel size of 16 × 16 μm^2. Excitation was provided by 491-nm light from a diode-pumped solid-state laser (Cobolt Calypso 100, Cobolt AG, Stockholm, Sweden) passing through a 490-nm bandpass filter (Chroma Technology Co.) and a 406 nm laser (Cube, Coherent). Pulses of 406-nm light (6−20 ms, 5−25 Hz) were passed through an acousto-optic modulator (AOM) (MT80-A3-VIS, AA Optoelectronic, Orsay, France), controlled by a function generator (USB-6218, National Instruments, Austin, TX). For the stroboscopic approach, the AOM was placed after the point at which the two beams were combined, providing simultaneous two-color pulses (6 ms, 25 Hz). Wide-field illumination was achieved by focusing the expanded and collimated laser beams onto the back-focal plane of the objective (Köhler illumination mode). The polarization of excitation light in the sample plane was tuned to be circular using zero-order $\lambda/4$ and $\lambda/2$ waveplates in order to compensate for polarization shift of the dichroic mirror. Emission was collected by the same objective and imaged by the CCD after passing through a dichroic mirror (z488rdc, Chroma Technology Co.) and additional spectral filters (HQ500LP, HQ530/60, Chroma Technology Co.), removing the excitation light and Raman scattering. The image was further magnified 3.3 times with a camera lens before the CCD camera, resulting in a maximum field of view of 24.6 × 24.6 μm^2 (48 × 48 nm^2 per pixel).

Analysis of the resulting images was performed with a homemade MATLAB routine, similarly to that previously described.[32]

Results and Discussion

Ensemble Spectroscopy. The steady-state absorption and emission spectra of Dronpa, Dronpa-2, and Dronpa-3 in PBS (pH 7.4) and the summary of their photophysical parameters are shown in Figure S1 (Supporting Information) and Table 1, respectively. Both absorption and fluorescence spectra of the mutants are shifted to the blue as compared to those of Dronpa. The extinction coefficients of the mutants at the absorption maximum are around half the value of Dronpa, which reflects a substantial perturbation of the electronic structure of the chromophore in the mutants. Values of Φ_F are also smaller for the mutants, probably reflecting a higher mobility of the chromophore in the β-can.[33] The fluorescence decays are more complex for the mutants as compared to Dronpa, with main components of 2.1 and 2.2 ns for Dronpa-2 and Dronpa-3, respectively (Table 1). Multiexponential fluorescence decays in GFP-like proteins have been associated in some cases to the higher flexibility of the chromophore in the protein environment and/or to the presence of different protein conformations.[34−37] For example, biexponential decays have been found for the cyan fluorescing protein variant with the Y66W mutation.[38] In this case, the two conformations arise from the different geometry of H148,[39,40] and a *cis−trans* isomerization process, resulting from an increased flexibility of the chromphore in the β-can, is thought to be responsible for a sub-nanosecond decay component.[34] In the case of DsRed, the super-red form produced after its photoconversion is characterized by a different hydrogen-bonding network and increased free volume around the chromophore. This allows the formation of a twisted configuration, which is reflected in the multiexponential fluorescence decay of the super-red form.[35] We propose a similar situation for Dronpa-2 and Dronpa-3, in which the two components in the nanosecond range correspond to two different conformations that might be in equilibrium in the ground state and/or interconverted in the excited state. The likely spectral similarity between the conformations precludes the discrimination between the two possibilities, since no rise component was found in the spectral range studied. The different conformations might arise

Table 1. Ensemble Photophysical Properties of Dronpa, Dronpa-2, and Dronpa-3 in Solution at pH 7.4

	Dronpa[a]	Dronpa-2	Dronpa-3
ϵ/M^{-1}·cm^{-1}	95 000	56 000	58 000
λ_{abs}^{max}/nm	503	486	487
λ_{fluo}^{max}/nm	518	513	514
Φ_F	0.85	0.28	0.33
Φ_{SW}[b]	3.2×10^{-4}	5×10^{-2}	5×10^{-3}
τ_F/ns[c]	3.6	2.1 (47%)	2.2 (66%)
		0.97 (42%)	1.1 (20%)
		0.09 (11%)	0.02 (14%)

[a] From refs 12 and 17. [b] From refs 12 and 16. [c] $\lambda_{ex} = 484$ nm.

(30) Maus, M.; Rousseau, E.; Cotlet, M.; Schweitzer, G.; Hofkens, J.; Van der Auweraer, M.; De Schryver, F.; Krueger, A. *Rev. Sci. Instrum.* **2001**, *72*, 36−40.
(31) Cotlet, M.; Hofkens, J.; Habuchi, S.; Dirix, G.; Van Guyse, M.; Michiels, J.; Vanderleyden, J.; De Schryver, F. C. *Proc. Natl. Acad. Sci. U.S.A.* **2001**, *98*, 14398−14403.
(32) Muls, B.; Uji-i, H.; Melnikov, S.; Moussa, A.; Verheijen, W.; Soumillion, J. P.; Josemon, J.; Mullen, K.; Hofkens, J. *ChemPhysChem* **2005**, *6*, 2286−2294.
(33) Follenius-Wund, A.; Bourotte, M.; Schmitt, M.; Iyice, F.; Lami, H.; Bourguignon, J. J.; Haiech, J.; Pigault, C. *Biophys. J.* **2003**, *85*, 1839−1850.
(34) Jung, G.; Wiehler, J.; Zumbusch, A. *Biophys. J.* **2005**, *88*, 1932−1947.
(35) Habuchi, S.; Cotlet, M.; Gensch, T.; Bednarz, T.; Haber-Pohlmeier, S.; Rozenski, J.; Dirix, G.; Michiels, J.; Vanderleyden, J.; Heberle, J.; De Schryver, F.; Hofkens, J. *J. Am. Chem. Soc.* **2005**, *127*, 8977−8984.
(36) Loos, D. C.; Habuchi, S.; Flors, C.; Hotta, J.; Wiedenmann, J. R.; Nienhaus, G. U.; Hofkens, J. *J. Am. Chem. Soc.* **2006**, *128*, 6270−6271.
(37) Cotlet, M.; Hofkens, J.; Maus, M.; Gensch, T.; Van der Auweraer, M.; Michiels, J.; Dirix, G.; Van Guyse, M.; Vanderleyden, J.; Visser, A. J. W. G.; De Schryver, F. C. *J. Phys. Chem. B* **2001**, *105*, 4999−5006.
(38) Hyun Bae, J.; Rubini, M.; Jung, G.; Wiegand, G.; Seifert, M. H.; Azim, M. K.; Kim, J. S.; Zumbusch, A.; Holak, T. A.; Moroder, L.; Huber, R.; Budisa, N. *J. Mol. Biol.* **2003**, *328*, 1071−1081.
(39) Seifert, M. H.; Ksiazek, D.; Azim, M. K.; Smialowski, P.; Budisa, N.; Holak, T. A. *J. Am. Chem. Soc.* **2002**, *124*, 7932−4792.
(40) Rizzo, M. A.; Springer, G. H.; Granada, B.; Piston, D. W. *Nat. Biotechnol.* **2004**, *22*, 445−449.

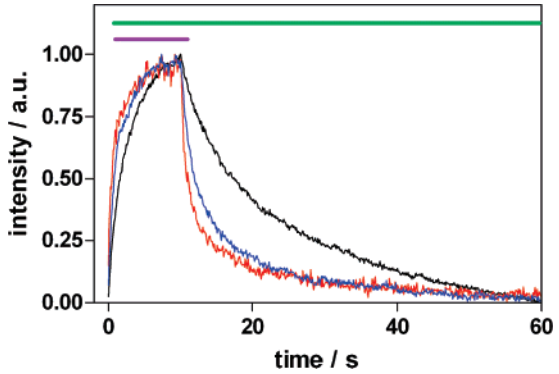

Figure 2. Response of Dronpa (black), Dronpa-2 (red), and Dronpa-3 (blue) (10^{-5}−10^{-6} M in PVA matrix) to 488-nm (green line) and 405-nm (violet line) light.

from different isomerization states or different twist angles between the five- and six-membered rings of the Dronpa chromophore (see Figure S2, Supporting Information). It is worth noting that both rings are slightly out of plane, with an angle of 7−15°.[15,41] On the other hand, the shortest decay time of tens of picoseconds may be attributed to the relaxation of the protein environment of the chromophore after photoexcitation, as suggested by femtosecond transient absorption spectroscopy results on Dronpa.[13]

As previously described, the quantum yield for forward photoswitching (Φ_{sw}) is higher for the mutants than for Dronpa.[16] In solution, Dronpa-2 ($\Phi_{sw} = 5 \times 10^{-2}$) switches an order of magnitude faster than Dronpa-3 ($\Phi_{sw} = 5 \times 10^{-3}$) and 2 orders of magnitude faster than Dronpa ($\Phi_{sw} = 3 \times 10^{-4}$). A similar trend can be observed in a PVA matrix (Figure 2), although the difference between Dronpa-2 and Dronpa-3 seems to be less pronounced, probably due to the interaction with the matrix. We can roughly estimate from Figure 2 that, in those conditions, the response to 488-nm light is 5 times faster for the mutants than for Dronpa.

The thermal recovery of the fluorescent state in the mutants is also faster than for Dronpa.[16] Indeed, we have measured the energy barrier for such thermal relaxation in Dronpa-2 as around 30 kJ·mol^{-1} in solution, much lower than the 109 kJ·mol^{-1} in Dronpa,[18] which reflects the effect of the different protein surroundings on the chromophore. This difference might allow a more accessible geometrical reorganization of the chromophore due to the less bulky amino acids at positions 157 or 159 and/or a more favorable hydrogen-bonding network in the mutants, thus facilitating the ground-state proton transfer involved in the recovery of the "on" state. We were unable to measure a reliable value for the energy barrier in Dronpa-3 in our experimental conditions due to its too-fast thermal recovery.

Photophysical Characterization at the Single-Molecule Level. Using confocal scanning microscopy, individual molecules of Dronpa-2 and Dronpa-3 immobilized in PVA can be imaged as reasonably bright spots using 488-nm light, despite their faster conversion to the "off" state as compared to Dronpa. Examples of single-molecule fluorescence trajectories of the three proteins in similar conditions (excitation 488 nm, 2 kW/cm^2) are shown in Figure 3. Dronpa (Figure 3a) shows several fluorescent bursts separated by a time interval in the order of seconds ("long off-times"), as reported before.[17] The presence of these bursts separated by long dark periods is rather common in Dronpa traces (between three and five bursts per trace on

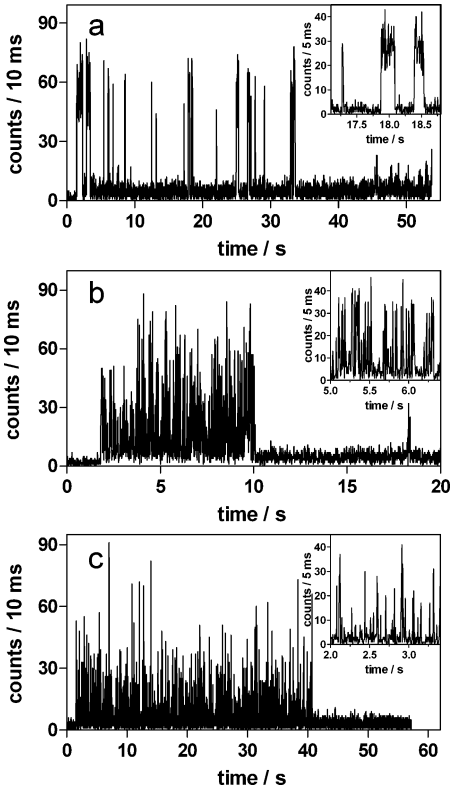

Figure 3. Single-molecule traces in PVA with 488-nm excitation (2 kW/cm^2) of (a) Dronpa, (b) Dronpa-2, and (c) Dronpa-3.

average), but less frequent in the case of Dronpa-2 and Dronpa-3 (one or two bursts per trace). We cannot reliably quantify the average "long off-time" due to the small amount of these events and to the fact that they will be biased to short times due to the intrinsic duration of our single-molecule experiments.[17]

The inset of Figure 3a shows one of the bursts in an expanded scale and reveals the presence of another on−off blinking process on a different time scale, around tens of milliseconds ("medium off-times").[17] The Dronpa-2 (Figure 3b) and Dronpa-3 (Figure 3c) traces show frequent on−off dynamics in this faster time scale. As mentioned in the Introduction, the long off-times are related to the slow dark recovery of the protonated form via intermediate I (k_2), and the medium off-times are associated with intermediate D (k_1). The presence of fewer long off-times and more medium off-times in the mutants as compared to Dronpa could be explained in two ways: (i) a different contribution of pathways 1 and 2 and/or (ii) a value of k_2 on the order of k_1, i.e., tens of milliseconds (Figure 1).

To unravel which of these possibilities best fits our observations, we statistically analyzed the on−off dynamics trajectories of 30−40 proteins of each type, comparing the results of one- and two-color experiments. The on-times from the one-color measurements (488 nm, 0.5 kW/cm^2) were histogrammed and could be fitted by monoexponential functions. In the case of Dronpa, the fit yielded an average on-time of 42 ms (Figure 4a). For the mutants, for which we expect much shorter on-times, the analysis was limited by the smallest bin time that could be used to obtain data with a reasonable signal-to-noise ratio (S/N) of 2 ms. Thus, Dronpa-2 and -3 have on-times equal to or smaller than ~2 ms, which is the fitted value in both panels b and c of Figure 5. These average on-times at the single-molecule level follow the tendency observed at the ensemble level.

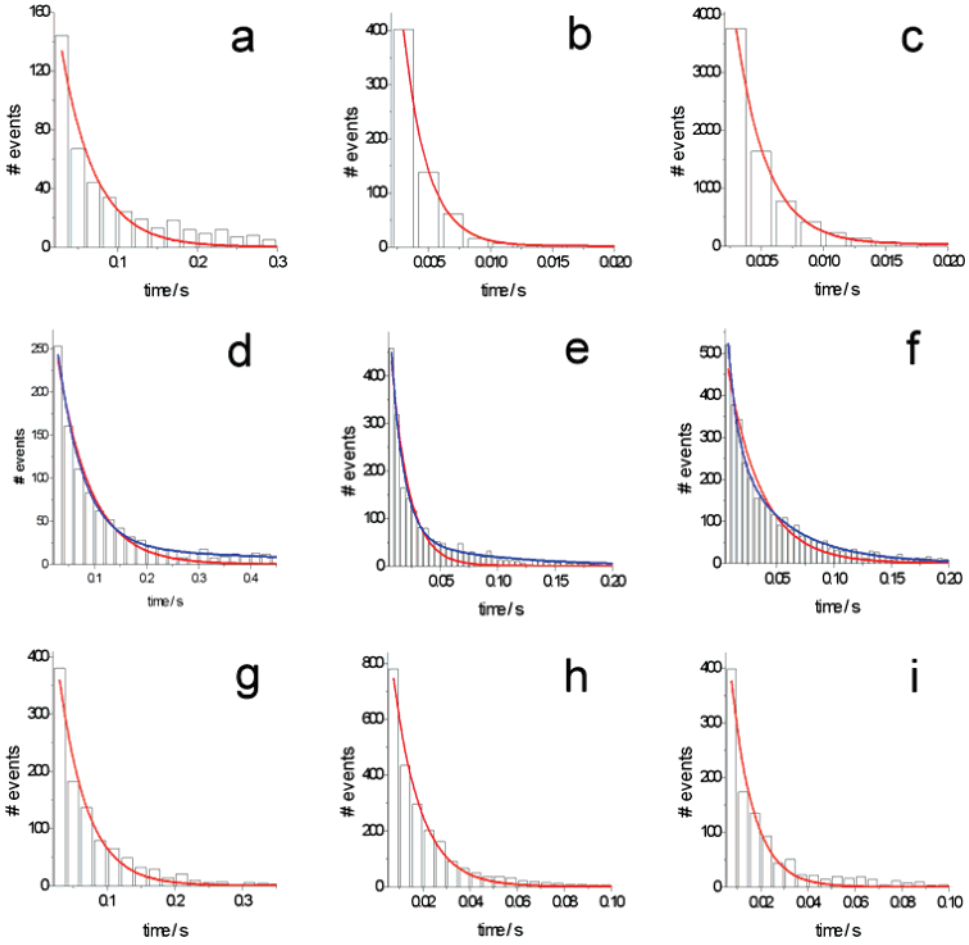

Figure 4. Frequency histograms constructed from one- and two-color experiments with monoexponential (red) or biexponential (blue) fits: (a−c) on-times in one-color experiment for Dronpa, Dronpa-2, and Dronpa-3, respectively; (d−f) off-times with one-color excitation for Dronpa, Dronpa-2, and Dronpa-3, respectively; (g−i) off-times with two-color excitation for Dronpa, Dronpa-2, and Dronpa-3, respectively.

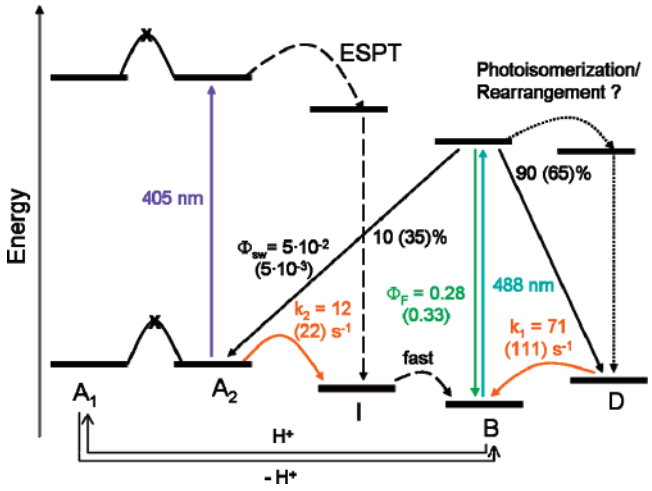

Figure 5. Photoconversion scheme for Dronpa-2 and Dronpa-3 in PVA. The values in parentheses correspond to Dronpa-3. Values for Φ_{sw} are those measured in solution. The dotted lines represent a hypothetical photoisomerization process.

As for the medium off-times from the one-color experiment, monoexponential functions were initially fitted to the histograms, although the quality of the fit was rather poor in the case of Dronpa-2 and Dronpa-3 (*vide infra*). The approximate average off-times were 63, 20, and 30 ms for Dronpa, Dronpa-2, and Dronpa-3, respectively (Figure 4d−f, red line). The introduction of 405 nm light (1 kW/cm^2) in the system results in the bypass of the thermal recovery process governed by k_2 (see Figure 1). Thus, the two-color experiments allow us to isolate the contribution of k_1 to the overall on−off dynamics. In this case, the recovered average off-times, corresponding to $1/k_1$, are 50, 11, and 9 ms for Dronpa, Dronpa-2, and Dronpa-3, respectively (Figure 4g−i). Comparing these time constants with those extracted from the one-color experiments, it can be noticed that the 405-nm light affects only slightly the off-time distribution of Dronpa, but considerably that of Dronpa-2 and Dronpa-3. This observation suggests that, in the latter case, there is a significant contribution of the two recovery processes (corresponding to k_1 and k_2) to the blinking dynamics in one-color excitation experiments. With the value of k_1 known, it is possible to discriminate between the two processes by fitting a biexponential function to the histograms from the one-color experiments (Figure 4d−f, blue line) with k_1 fixed and equal to the value found above. In this case, the fits are much better than with monoexponential functions for Dronpa-2 and Dronpa-3 and result in off-time constants ($1/k_2$) of 80 ms (∼10% amplitude) and 46 ms (∼35% amplitude), respectively, with the amplitude corresponding to the relative contribution of pathway 2.

The values of k_2 extracted from the single-molecule experiments are consistent with the behavior of the three proteins in solution; i.e., the thermal recovery of Dronpa-3 is faster than that of Dronpa-2, and both recover orders of magnitude faster

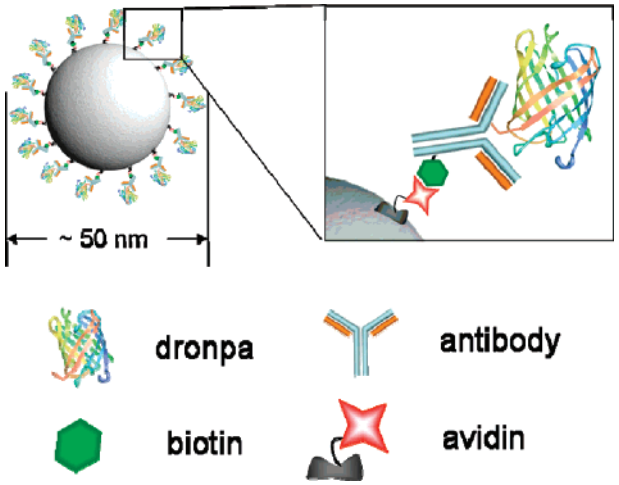

Figure 6. Schematic representation of Dronpa-coated spheres.

than Dronpa. Figure 5 summarizes the photoswitching scheme for Dronpa-2 and Dronpa-3 and includes the rate constants and relative contributions of the different pathways. It is evident from this scheme that, besides the higher values of k_1 and especially k_2, there is also a difference in the relative contribution of each pathway. The higher contribution of pathway 1 in the mutants might be related to the higher flexibility of the chromophores in the β-can that has been evidenced in the experiments presented above; i.e., pathway 1 is a process that is hindered by a tight geometry of the chromophore. It has been suggested that smaller amino acids at positions 157 and 159 in Dronpa mutants may allow *cis*−*trans* isomerization of the chromophore.[15,41] Residue 159 can potentially interfere with the mobility of the chromophore, precluding the movement of the six-membered ring upon isomerization.[15] In these mutants, smaller residues like threonine (Dronpa-2) and alanine (Dronpa-3) replace a methionine at this position. Thus, our observation suggests that intermediate D might be an isomerized form of the chromophore arising from *cis*−*trans* rearrangement (pathway 1). The effect of the new OH group of the threonine in Dronpa-2 is not clear at this point, but it might be close enough to the tyrosyl ring of the chromophore to influence the H-bonding network.

Photoactivation−Localization Microscopy. With the rate constants for switching in hand, we set out to use Dronpa and its mutants for camera-based sub-diffraction-limit imaging. We used a sample containing nanospheres of known diameter coated with Dronpa and Dronpa-3 (∼50 nm, see Materials and Methods and Figure 6) immobilized in PVA to be able to provide an estimation of the quality of our reconstructed PALM images. Figure 7 shows the reconstructed sub-diffraction-limit images of the nanospheres, in which two different approaches were used to acquire the data. In the first case (panels a−d), continuous illumination with 491-nm light and pulsed 406-nm light was applied. The 491-nm laser power was equivalent to that used in the single-molecule confocal study (around 0.5 kW/cm^2), and the 406-nm power ranged from 4 to 30 W/cm^2. For Dronpa (panels a and b), the integration time per frame was tuned to its average on-time of ∼40 ms. The frequency of 406-nm pulses (5 Hz, 20 ms) was chosen to allow enough time for the dark

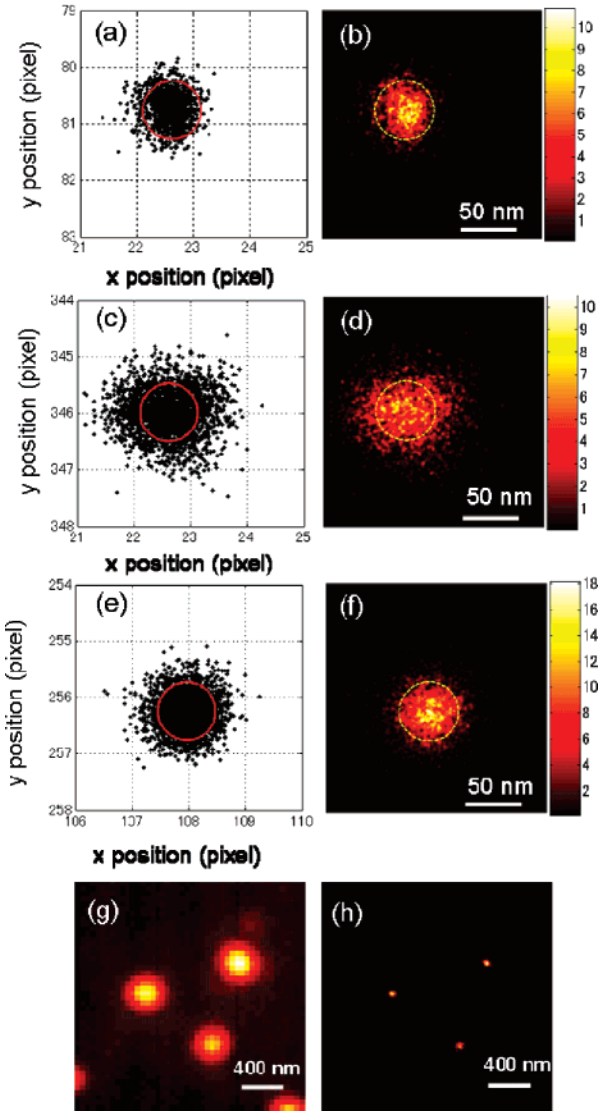

Figure 7. Reconstructed PALM images (491-nm continuous and 406-nm pulsed excitation, 40 ms/frame) of nanospheres coated with Dronpa (a,b) and Dronpa-3 (c,d). S-PALM reconstructed images of Dronpa-3 spheres with 6 ms simultaneous two-color illumination per frame (e,f). Each square in the grid represents the size of 1 pixel, and the circles correspond to a diameter of 50 nm. Panels g and h depict the accumulated and reconstructed S-PALM images, respectively, of a larger sample area showing three spheres coated with Dronpa-3.

state D to relax ($1/k_1$ = 66 ms, Figure 1), and the 406-nm power was increased as the experiment progressed.[25] With these optimal parameters, it was possible to obtain individual fluorescent Dronpa molecules with enough S/N to allow precise localization (<15 nm) with our fitting routine (see Figure S3, Supporting Information). After the acquisition of 3000 frames, the reconstructed images indeed show the expected dimensions of the nanospheres, i.e., the 50-nm diameter shown as a circle in panels a and b, with few data points outside the circle. This corresponds to a resolution improvement of approximately $\lambda/10$. For comparison, we found that we could localize an isolated individual Dronpa molecule repeatedly over the course of the measurement, yielding an identical position within the fitting error (Figure 8). This finding demonstrates that the experimental setup is sufficiently stable over the duration of the measurement and that the images of the localized spheres are physically

(41) Wilmann, P. G.; Turcic, K.; Battad, J. M.; Wilce, M. C. J.; Devenish, R. J.; Prescott, M.; Rossjohn, J. *J. Mol. Biol.* **2006**, *364*, 213−224.

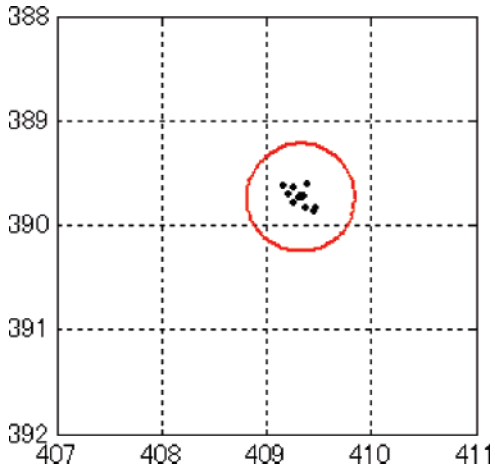

Figure 8. Localization of a single Dronpa molecule in the same experimental conditions as in Figure 7a,b. A total of 12 data points were detected for this molecule, which are localized within the fitting error. The red circle represents a 50-nm-diameter circle.

relevant. The spheres contain a maximum of only ~170 Dronpa molecules (see Materials and Methods), but due to the reversible properties of Dronpa, the image could be constructed with more than 1000 data points, providing a more accurate picture of the sample. This is an important factor that should be taken into consideration when choosing between reversible or irreversible photoactivatable fluorophores. Depending on the nature of the sample and on the information in which one is interested, reversibility might be much more advantageous, since it allows one to probe the same molecule several times.

The total acquisition time was 120 s, which is fast enough to ensure that no correction for sample drift is needed (provided that the system is allowed to mechanically stabilize before the experiment). This fast acquisition time is orders of magnitude lower than those reported for PALM images with other fluorescent proteins[25] and about one-third of that reported in STORM[27] and FPALM,[26] which implies that common equipment (in terms of mechanical stability) can be used. Moreover, no external markers such as quantum dots or fluorescent beads are needed to correct the position coordinates, which is an advantage for the sample preparation step. The actual measurement time will, however, depend on the complexity of the sample under study.

The experiment was also carried out with spheres coated with the mutant Dronpa-3 using the same acquisition parameters as for Dronpa (40 ms per frame). As judged from Figure 7 (panels c and d), the data points are more scattered outside the circle that defines the 50-nm diameter. The higher scattering is a consequence of lower S/N, which yields less accurate Gaussian fits of the single molecules (Figure S3). In order to compare the scattering of the data points in the experiments on Dronpa and Dronpa-3, we fitted once again a Gaussian function to a line profile of the spheres (Figure S3, columns A and B). The width of the Gaussian is larger for Dronpa-3 than for Dronpa, which serves as an indication of the higher spread of the data points. However, it is important to note that the values of the full width at half-maximum (fwhm) given in Figure S4 are neither a direct measure of the size of the bead nor of the resolution of our images, and fwhm is just a parameter that allows comparison between the experiments presented herein.

There are two reasons for the poorer S/N: (i) the lower Φ_F for Dronpa-3 (0.33) compared to that of Dronpa (0.85) and (ii) the much lower average on-time for Dronpa-3 than for Dronpa (2 vs 42 ms), which implies that the integration time per frame (40 ms) is too long; i.e., the CCD camera will be, on average, measuring noise 95% of the time. Thus, we explored whether a shorter integration time tuned to the average on-time of Dronpa-3 would be an advantage. Since our CCD camera cannot provide integration times of a few milliseconds, we kept the integration time to 40 ms but only illuminated the sample during the calculated average on-time in order to reduce the background to a minimum during the 95% of the time that the molecules are in their their dark state.[42] This approach can be compared to stroboscopic photography, in which short light flashes allow a fast moving object to be followed while the shutter of the camera remains open. We have thus termed this new approach stroboscopic (S)-PALM. For S-PALM, a different configuration of the setup was used (see Materials and Methods), resulting in lower excitation power (around 0.17 kW/cm^2) at the sample. In this configuration, the AOM controlled both beams at the same time, which resulted in two-color simultaneous irradiation. It had been shown before that simultaneous two-color irradiation of Dronpa-3 is preferable for imaging, providing fast cycling between its bright and dark states.[16] The excitation power used is 3 times lower than in the experiments described above, and since the on-time is linearly dependent on the power,[17] we expect the latter parameter to be around 6 ms. Thus, the illumination time was set to 6 ms, with a frequency of 25 Hz (matching the integration time of the camera of 40 ms). This frequency also allowed the state D to fully relax back to B ($1/k_1 = 9$ ms) before the next pulse arrived (see Figure 5). The result of S-PALM on Dronpa-3 is shown in Figure 7 (panels e and f), which consists of the reconstructed images after 3000 frames. It is clear from this figure that localization is more precise and that the number of points scattered outside the circle is reduced as compared to panels c and d (see also Figure S4C). Figure 7 also shows the accumulated (panel g) and S-PALM reconstructed image (panel h) of a larger area of the CCD image, in which the resolution improvement is more evident.

Our results provide a proof-of-principle of the stroboscopic approach, which relies on the possibility of pulsing the light rather than on a fast CCD camera. In the case of the availability of a faster CCD camera, it is possible to reduce total acquisition times further by using Dronpa-3, only keeping in mind that the dark state D relaxes with a time constant of 9 ms. Indeed, during the preparation and review of this manuscript, two papers were released describing PALM with the Dronpa mutant rsFastLime and a specially designed photochromic rhodamine dye in which integration times of 2−10 ms were used.[28,43,44] However, S-PALM is a useful alternative that can be easily implemented in existing wide-field setups.

In practice, the choice between using Dronpa or one of the Dronpa mutants in these experiments will depend on the particular system to be investigated; i.e., Dronpa provides more

(42) Elf, J.; Li, G. W.; Xie, X. S. *Science* **2007**, *316*, 1191−1194.
(43) Geisler, C.; Schönle, A.; von Middendorff, C.; Bock, H.; Eggeling, C.; Egner, A.; Hell, S. W. *Appl. Phys. A: Mater.* **2007**, *88*, 223−226.
(44) Folling, J.; Belov, V.; Kunetsky, R.; Medda, R.; Schonle, A.; Egner, A.; Eggeling, C.; Bossi, M.; Hell, S. W. *Angew. Chem., Int. Ed.* **2007**, *46*, 6266−6270.

photons, allowing more precise localization (Figure S3), while Dronpa-3 allows for faster imaging.

Conclusion

The data collected from both ensemble and single-molecule experiments on three reversible photoswitchable proteins, Dronpa, Dronpa-2, and Dronpa-3, have allowed us to unravel the differences in the rate constants and efficiencies of the processes involved in their forward and backward photoswitching. The faster response to light in the forward photoswitching of Dronpa-2 and -3 is confirmed at the single-molecule level, as well as the faster thermal recovery from the "off" state to the "on" state. The faster rate constants for recovery, a consequence of an 80 $kJ \cdot mol^{-1}$ difference in energy barriers, underscore the impact of changing only one or two residues around the chromophore. Our ensemble and single-molecule results point to the existence of higher conformational freedom of the chromophore in Dronpa-2 and -3. The higher contribution of pathway 1 in the mutants allows us to speculate that the dark intermediate D is a form of the chromophore arising from *cis*−*trans* isomerization.

With the knowledge of the photoswitching rates, which allow us to optimize the acquisition parameters for camera-based sub-diffraction-limit imaging, we have also shown that Dronpa and its mutants are useful for fast PALM and that their reversibility properties offer advantages in terms of the number of data points that can be obtained. We have introduced a new approach for PALM that relies on two-color simultaneous stroboscopic illumination (S-PALM). This approach is valuable when dealing with very fast switching fluorophores (Dronpa-3 in this case) and is not limited by the requirement of fast CCD cameras. Alternatively, if faster integrations times per frame can be achieved, total acquisition times can be reduced even more by the use of Dronpa mutants, thus allowing the study of dynamic processes in live cells.

Acknowledgment. Support from the FWO (grant G.0366.06), the KU Leuven Research Fund (GOA 2006/2, CREA 2007, Center of Exellence INPAC through a postdoctoral fellowship to C.F.), the Flemish Ministry of Education (ZWAP 04/007), and the Federal Science Policy of Belgium (IAP-VI) is gratefully acknowledged. P.D. is a fellow of the Fonds voor Wetenschappelijk onderzoek (aspirant van het FWO). This work, as part of the European Science Foundation EUROCORES Program SONS, was supported by funds from the FWO and the EC 6th Framework Program (ERAS-CT-2003-980409). We thank Ania Deres for technical help with the wide-field setup.

Supporting Information Available: Absorption and emission spectra of Dronpa, Dronpa-2, and Dronpa-3; fitting error and S/N histograms and line profiles corresponding to Figure 7; chemical structure of the chromophore in Dropna. This material is available free of charge via the Internet at http://pubs.acs.org.

JA074704L